Original Research Paper

Volume - 13 | Issue - 01 | January - 2023 | PRINT ISSN No. 2249 - 555X | DOI : 10.36106/ijar

Mathematics

BUCKLING REGIMES IN BINGHAM PLASTICS FLOW IN AN ECCENTRIC INNER PIPE INSIDE A VERTICAL CLOSED-END OUTER PIPE

P.Srinivasa Sai*	Department of Mathematics, S.S&N College,Narasaraopet, Palnadu Dist. A.P, India. *Corresponding Author
A. Subba Rao	Department of Physics , S.S&N College, Narasaraopet, palnadu Dist, A.P, India.
J.Manjula	Department of Mathematics , T.S.W.R.D.C – Khammam, Telangana , India.
K.Venugopal Reddy	Department of Mathematics, Malla Reddy Engineering college (Autonomous), Maisammaguda, Hyderabad, Telangana 500100, India.

ABSTRACT We develop a lubrication approximation model, using the Herschel–Bulkley constitutive equation, with dimensionless flow parameters including the Bingham number, the power-law index, the buoyancy number, the viscosity ratio, the diameter ratio, the eccentricity and the aspect ratio. Based on a reasonable prediction to the yielding onset, the model allows us to classify the flow regimes versus an elegant combination of the dimensionless numbers. We study the injection flow of a heavy viscoplastic fluid into a light Newtonian fluid, via modelling and experiments. The injection is carried out downward, via an eccentric inner pipe inside a vertical closed-end outer pipe. This configuration results in a core viscoplastic fluid surrounded by an annular Newtonian fluid. The flow is structured and mixing is negligible. As the injection rate increases in a typical experiment, we observe three distinct flow regimes, associated with the core fluid behavior, namely the breakup, coiling and buckling (bulging) regimes.

KEYWORDS :

1. Introduction:

The injection of a viscoplastic fluid into another fluid occurs in many industrial applications, such as the plug and abandonment (P&A) of oil and gas wells (Nelson & Guillot Reference Nelson and Guillot2006; Khalifeh &Saasen Reference Khalifeh and Saasen2020; Akbari &Taghavi Reference Akbari and Taghavi2021), three-dimensional printing (Karyappa, Ohno & Hashimoto Reference Karyappa, Ohno and Hashimoto2019; Lawson et al. Reference Lawson, Li, Thakkar, Rownaghi and Rezaei2021), etc. From a fluid mechanics perspective, analysingviscoplastic fluid injection processes comes down to quantifying the interface evolution between the fluids, in particular in terms of the yielding behaviour of the viscoplastic fluid (Bonn et al. Reference Bonn, Denn, Berthier, Divoux and Manneville2017; Frigaard Reference Frigaard2019). However, the flow analysis may be complex, due to the presence of a large number of flow parameters, e.g. the density and viscosity ratios, the flow geometry characteristics and the yield stress, resulting in a variety of flow patterns, e.g. breakup, coiling, dripping and buckling of viscoplastic fluids (Balmforth, Frigaard&Ovarlez Reference Balmforth, Frigaard and Ovarlez2014).

2. Litterature survey:

Previous works have mainly considered the dynamics of a viscoplastic fluid injected/extruded under gravity into a dynamically passive exterior fluid, i.e. typically air. In this context, a dynamically passive fluid represents an exterior fluid that is assumed to remain stagnant or whose flow is assumed not to affect the injected fluid flow; in fact, only the exterior fluid's physical properties (e.g. the surface tension with the injected fluid) may affect the injected fluid flow dynamics. On the other hand, a dynamically active fluid, which is in direct contact with the injected fluid at the interface, describes a medium whose flow accompanied by its physical properties exerts significant forces on the injected fluid and, consequently, alters the flow dynamics. For example, Coussot&Gaulard (Reference Coussot and Gaulard2005) have experimentally and theoretically investigated the breakup of an extruded viscoplastic fluid into air, finding that an unyielded layer is developed until its weight becomes larger than the yield stress force; this leads to the yielding and breakup of the layer, forming a droplet, the volume of which increases with increasing flow rate. Similar results have been obtained by Al Khatib & Wilson (Reference Al Khatib and Wilson2005).

3. Mathematical Formulation:

We consider an incompressible viscoplastic core fluid, which follows the HB constitutive model, and an annular fluid, which is Newtonian. Since our problem involves non-coaxial cylinders (eccentric annuli), we use the bipolar coordinates (ξ,□,z)Let us consider the peristaltic transport of an incompressible Newtonian Fluid flow in an inclined asymmetric channel of half-width a. The angle of inclination is . A sinusoidal wave propagating with constant speed c on the channel walls induces the flow. The geometry of the wall surface is defined as

$$Y = H = a + b\sin\left[\frac{2\pi}{\lambda}\left(\bar{X} - c\bar{t}\right)\right] \tag{3.1}$$

Under the assumption that the channel length is an integral multiple of the wavelength λ and the pressure difference across the ends of the channel is a constant, the flow becomes steady in the wave frame moving with velocity c away from the fixed frame. The transformation between these two frames is defined by

$$\bar{x} = X - ct \quad , \bar{y} = Y \quad ; \bar{u} = U - c, \ \bar{v} = V \ , and \ \ \bar{p}(x) = P(X,t) \tag{3.2}$$

Where (u, v) and (U, V) are the velocity components, p and P are pressures in the wave and fixed frames of reference, respectively.
The equations governing the flow are given by

$$\frac{\partial \bar{u}}{\partial x} + \frac{\partial \bar{v}}{\partial y} = 0 \tag{3.3}$$

$$\rho\left(u\frac{\partial u}{\partial x} + v\frac{\partial u}{\partial y}\right) = -\frac{\partial p}{\partial x} + \mu\left(\frac{\partial^2 u}{\partial x^2} + \frac{\partial^2 u}{\partial y^2}\right) - \frac{\sigma B_0^2}{1+m^2}(mv - (u+c)) + \rho g \sin\alpha \tag{3.4}$$

$$\rho\left(u\frac{\partial u}{\partial x} + v\frac{\partial u}{\partial y}\right) = -\frac{\partial p}{\partial y} + \mu\left(\frac{\partial^2 v}{\partial x^2} + \frac{\partial^2 v}{\partial y^2}\right) - \frac{\sigma B_0^2}{1+m^2}(m(u+c) + v) - \rho g \cos\alpha \tag{3.5}$$

Where p is the density, is the electrical conductivity, B_0 is the magnetic field strength and is the Hall parameter.
The dimensional boundary conditions are

$$u = -c \quad at \quad y = H \tag{3.6}$$

$$\frac{\partial u}{\partial v} = 0 \ at \quad y = 0 \tag{3.7}$$

Introducing the non-dimensional quantities

$$\bar{x} = \frac{x}{\lambda}, \bar{y} = \frac{y}{a}, \bar{u} = \frac{u}{c}, \bar{v} = \frac{v}{c\delta}, \delta = \frac{a}{\lambda}, \bar{p} = \frac{a^2}{\mu c\lambda}, \bar{t} = \frac{ct}{\lambda}, h = \frac{H}{a}, \phi = \frac{b}{a}, \bar{q} = \frac{q}{ac}, M^2 = \frac{\sigma a^2 B_0^2}{\mu} \tag{3.8}$$

From the equations (3.3) to (3.5), we get

$$\frac{\partial u}{\partial x} + \frac{\partial v}{\partial y} = 0 \tag{3.9}$$

$$Re\,\delta\left(u\frac{\partial u}{\partial x} + v\frac{\partial u}{\partial y}\right) = -\frac{\partial p}{\partial x} + \left(\delta^2\frac{\partial^2 u}{\partial x^2} + \frac{\partial^2 u}{\partial y^2}\right) + \frac{M^2}{1+m^2}(m(v-(u+1)) + \frac{Re}{Fr}\sin\alpha \tag{3.10}$$

$$Re\,\delta^2\left(u\frac{\partial v}{\partial x} + v\frac{\partial v}{\partial y}\right) = -\frac{\partial p}{\partial y} + \delta^2\left(\delta^2\frac{\partial^2 v}{\partial x^2} + \frac{\partial^2 v}{\partial y^2}\right) - \frac{\delta M^2}{1+m^2}(m(u+1) + \delta v) + \frac{\delta Re}{Fr}\cos\alpha \tag{3.11}$$

Where $Fr=\frac{c^2}{ag}$ is the Froude number, is the Hartmann number and is the Reynolds number. Using long wavelength i.e. is less than 1, approximation, the equations (3.10) and (3.11) become

$$\frac{\partial^2 u}{\partial y^2} \quad \frac{M^2}{1+m^2}u \quad \frac{\partial p}{\partial x} \quad \frac{\mathrm{Re}}{Fr}\sin\alpha + \frac{M^2}{1+m^2} \qquad (3.12)$$

$$\frac{\partial p}{\partial y} - 0 \qquad (3.13)$$

From equation (3.13), it is clear that p is independent of y .Therefore equation (3.12) can be rewritten as

$$\frac{\partial^2 u}{\partial y^2} \quad \frac{M^2}{1+m^2}u \quad \frac{dp}{dx} \quad \frac{\mathrm{Re}}{Fr}\sin\alpha + \frac{M^2}{1+m^2} \qquad (3.14)$$

The corresponding non-dimensional boundary conditions are given as

u=-1 at y=H (3.15)

$$\frac{\partial u}{\partial y} = 0 \text{ at } \quad y=0 \qquad (3.16)$$

Knowing the velocity, the volume flow rate q in a wave frame of reference is given by

$$Q-\int_0^h u dy \qquad (3.17)$$

The instantaneous flow $Q(X,t)$ in the laboratory frame is

$$Q(X,t)\int_0^h U dY - \int_0^h (u+1)dy - q+h \qquad (3.18)$$

The time averaged volume flow rate Q over one period $T-\frac{\lambda}{c}$ of the peristaltic wave is given by

$$Q-\frac{1}{T}\int_0^T Q dt - q+1 \qquad (3.19)$$

3.3. Solution of the Problem:

Solving equation (3.14) together with the boundary conditions (3.15) and (3.16), we get

$$u=\frac{1}{\beta^2}\left(\frac{dp}{dx}-\frac{\mathrm{Re}}{Fr}\sin\alpha\right)\left[\frac{\cosh\beta y}{\cosh\beta h}-1\right]-1 \qquad (3.20)$$

where $\beta = M/\sqrt{1+m^2}$

4. Graphical Representation:

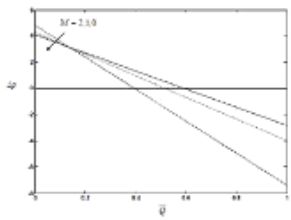

Fig. 1

Variation of pressure rise Δp with time -averaged flow rate $\bar{Q}$ for different values of Hartmann number M with $\phi=0.5, \mathrm{Re}=5, \alpha=\frac{\pi}{4}, Fr=2$ and $m=0.2$

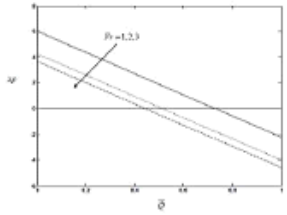

Fig. 2

Variation of pressure rise Δp with time-averaged flow rate Q for different values of Froude number Fr with $\phi=0.5, \mathrm{Re}=5, \alpha=\frac{\pi}{4}, m=0.2$ and $M=1$

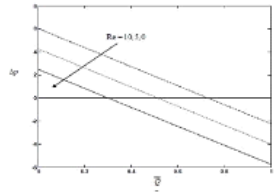

Fig. 3

Variation of pressure rise Δp with time-averaged flow rate Q for different values of Reynolds number Re with $\phi=0.5, Fr=2, \alpha=\frac{\pi}{4}, m=0.2$ and $M=1$.

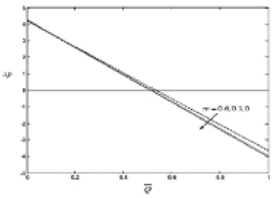

Fig.4

Variation of pressure rise Δp with time-averaged flow rate Q for different values of Hall parameter m with $\phi=0.5, \mathrm{Re}=5, \alpha=\frac{\pi}{4}, Fr=2$ and $M=1$.

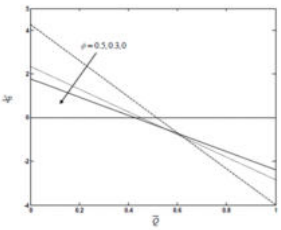

Fig.5

Variation of pressure rise Δp with time-averaged flow rate Q for different values of amplitude ratio ϕ with $\alpha=\frac{\pi}{4}, \mathrm{Re}=5, \mathrm{Re}=5, m=0.2$ and $M=1$.

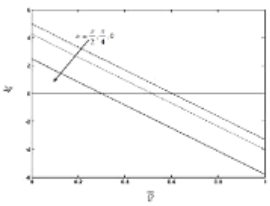

Fig. 6

Variation of pressure rise Δp with time-averaged flow rate $\bar{Q}$ for different values of inclination angle α with ϕ 0.5,Re 5,Re 5,m 0.2 and $M=1$

5. Results & Discussion:

1. It is found that, the time-averaged flow rate increases in the pumping region is positive with increasing , while it decreases in both the free-pumping is equal to 0 and co-pumping is negative regions with increasing .
2. It is observed that as increase in decreases the time averaged flow rate in all the pumping, free -pumping and co-pumping regions.
3. It is found that, on increasing increases the time averaged flow rate in all the pumping, free-pumping and co-pumping regions.
4. It is observed that, the time-averaged flow rate decreases in the pumping region with an increase in , while it increases in both the free -pumping and co-pumping regions with increasing .
5. It is observed that, the time-averaged flow rate increases with increasing amplitude ratio in both the pumping and free pumping regions.
6. It is also observed that decreases with increasing amplitude ratio in the co-pumping region for chosen.
7. It is noticed that, the time averaged flow rate increases with increasing in all the pumping, free-pumping and co-pumping regions.

6. REFERENCES:

[1] Jalaal, M. 2016 Controlled spreading of complex droplets. PhD thesis, University of British Columbia.Google Scholar
[2] Jalaal, M., Balmforth, N.J. & Stoeber, B. 2015 Slip of spreading viscoplastic droplets. Langmuir 31 (44), 12071–12075.CrossRefGoogle ScholarPubMed
[3] Jalaal, M., Kemper, D. & Lohse, D. 2019 Viscoplastic water entry. J. Fluid Mech. 864, 596–613.CrossRefGoogle Scholar
[4] Jalaal, M., Stoeber, B. & Balmforth, N.J. 2021 Spreading of viscoplastic droplets. J. Fluid Mech. 914, A21.CrossRefGoogle Scholar
[5] Jaworski, Z., Spychaj, T., Story, A. & Story, G. 2021 Carbomer microgels as model yield-stress fluids. Rev. Chem. Engng, https://doi.org/10.1515/revce-2020-0016.CrossRefGoogle Scholar
[6] Jørgensen, L., Le Merrer, M., Delanoë-Ayari, H. & Barentin, C. 2015 Yield stress and elasticity influence on surface tension measurements. Soft Matt. 11 (25), 5111–5121.CrossRefGoogle ScholarPubMed
[7] Karyappa, R., Ohno, A. & Hashimoto, M. 2019 Immersion precipitation 3D printing (ip 3DP). Mater. Horiz. 6 (9), 1834–1844.CrossRefGoogle Scholar
[8] Khalifeh, M. & Saasen, A. 2020 Introduction to Permanent Plug and Abandonment of Wells. Springer Nature.CrossRefGoogle Scholar
[9] Kordalis, A., Varchanis, S., Ioannou, G., Dimakopoulos, Y. & Tsamopoulos, J. 2021 Investigation of the extensional properties of elasto-visco-plastic materials in cross-slot

geometries. J. Non-Newtonian Fluid Mech. 296, 104627.CrossRefGoogle Scholar
[10] Lawson, S., Li, X., Thakkar, H., Rownaghi, A.A. & Rezaei, F. 2021 Recent advances in 3D printing of structured materials for adsorption and catalysis applications. Chem. Rev. 121 (10), 6246–6291.CrossRefGoogle ScholarPubMed
[11] Leal, L.G. 2007 Advanced Transport Phenomena: Fluid Mechanics and Convective Transport Processes. Cambridge University Press.CrossRefGoogle Scholar
[12] Moschopoulos, P., Syrakos, A., Dimakopoulos, Y. & Tsamopoulos, J. 2020 Dynamics of viscoplastic filament stretching. J. Non-Newtonian Fluid Mech. 284, 104371.CrossRefGoogle Scholar
[13] Nelson, E.B. & Guillot, D. 2006 Well Cementing, 2nd edn. Schlumberger Educational Services.Google Scholar
[14] O'Bryan, C.S., BradyMiné, A., Tessmann, C.J., Spotz, A.M. & Angelini, T.E. 2021 Capillary forces drive buckling, plastic deformation, and break-up of 3D printed beams. Soft Matt. 17 (14), 3886–3894.CrossRefGoogle ScholarPubMed
[15] Ovarlez, G., Barral, Q. & Coussot, P. 2010 Three-dimensional jamming and flows of soft glassy materials. Nat. Mater. 9 (2), 115–119.CrossRefGoogle ScholarPubMed
[16] Pan, K., Phani, A.S. & Green, S. 2020 Periodic folding of a falling viscoelastic sheet. Phys. Rev. E 101 (1), 013002.CrossRefGoogle ScholarPubMed
[17] Pereira, A., Hachem, E. & Valette, R. 2020 Inertia-dominated coiling instabilities of power-law fluids. J. Non-Newtonian Fluid Mech. 282, 104321.CrossRefGoogle Scholar
[18] Pereira, A., Larcher, A., Hachem, E. & Valette, R. 2019 Capillary, viscous, and geometrical effects on the buckling of power-law fluid filaments under compression stresses. Comput. Fluids 190, 514–519.CrossRefGoogle Scholar
[19] Rahmani, Y., Habibi, M., Javadi, A. & Bonn, D. 2011 Coiling of yield stress fluids. Phys. Rev. E 83 (5), 056327.CrossRefGoogle ScholarPubMed
[20] Rahmani, H. & Taghavi, S.M. 2020 Linear stability of plane Poiseuille flow of a Bingham fluid in a channel with the presence of wall slip. J. Non-Newtonian Fluid Mech. 282, 104316.CrossRefGoogle Scholar
[21] Rasschaert, F., Talansier, E., Blésès, D., Magnin, A. & Lambert, M. 2018 Packaging of yield stress fluids: flow patterns. AlChE J. 64 (3), 1117–1126.CrossRefGoogle Scholar
[22] Ribe, N.M. 2001 Bending and stretching of thin viscous sheets. J. Fluid Mech. 433, 135–160.CrossRefGoogle Scholar
[23] Ribe, N.M. 2003 Periodic folding of viscous sheets. Phys. Rev. E 68 (3), 036305.CrossRefGoogle ScholarPubMed
[24] Ribe, N.M. 2004 Coiling of viscous jets. Proc. R. Soc. Lond. Ser. A: Math. Phys. Engng Sci. 460 (2051), 3223–3239.CrossRefGoogle Scholar
[25] Ribe, N.M. 2017 Liquid rope coiling: a synoptic view. J. Fluid Mech. 812, R2.CrossRefGoogle Scholar
[26] Ribe, N.M., Habibi, M. & Bonn, D. 2012 Liquid rope coiling. Annu. Rev. Fluid Mech. 44, 249–266.CrossRefGoogle Scholar
[27] Roberts, G.P. & Barnes, H.A. 2001 New measurements of the flow-curves for Carbopol dispersions without slip artefacts. Rheol. Acta 40 (5), 499–503.CrossRefGoogle Scholar
[28] Sica, L.U.R., de Souza Mendes, P.R. & Thompson, R.L. 2020 Is the von Mises criterion generally applicable to soft solids? Soft Matt. 16 (32), 7576–7584.CrossRefGoogle ScholarPubMed
[29] Taghavi, S.M. 2018 A two-layer model for buoyant displacement flows in a channel with wall slip. J. Fluid Mech. 852, 602–640.CrossRefGoogle Scholar
[30] Taghavi, S.M., Seon, T., Martinez, D.M. & Frigaard, I.A. 2009 Buoyancy-dominated displacement flows in near-horizontal channels: the viscous limit. J. Fluid Mech. 639, 1–35.CrossRefGoogle Scholar